arXiv:1701.08136v1 [cond-mat.supr-con] 27 Jan 2017

Materials' specific theory expounding high-temperature superconductivity in monolayer FeSe/$SrTiO_3$

Alex Aperis* and Peter M. Oppeneer†
Department of Physics and Astronomy, Uppsala University, P. O. Box 516, SE-75120 Uppsala, Sweden
(Dated: January 30, 2017)

Superconductivity in monolayer-thick FeSe on $SrTiO_3$ reaches amazingly high transition temperatures of typically T_c=50–70 K [1–6] and up to 100 K [7], much higher than the 8-K value of bulk FeSe [8]. A coupling between $SrTiO_3$ phonons and FeSe electrons occurs at the FeSe/$SrTiO_3$ interface, which manifests itself as electron replica bands [6]. This coupling is commonly believed to enhance T_c moderately but not be enough to explain it [6, 9, 10]. Here, we examine the impact of interfacial phonons on the superconducting state of FeSe/$SrTiO_3$ developing anisotropic, full bandwidth, multiband Eliashberg theory. Our selfconsistent calculations prove that the interfacial electron-phonon interaction which is hidden behind a seemingly weak coupling constant, λ_m=0.4 [6, 10], fully explains the high-T_c as well as puzzling experimental observations like the s-wave symmetry and replica bands. We find that deep Fermi-sea Cooper pairing has a T_c enhancing effect whereas replica-band formation has a decreasing effect. We predict a strong coupling dip-hump signature in the tunneling spectra due to the interfacial coupling.

The superconducting state in iron-based superconductors is customarily associated with residual spin fluctuations due to the remnant quasi-nesting between electron and hole Fermi sheets that give rise to a sign alternating gap [11]. However, for FeSe/STO the situation is markedly different. Charge transfer at the interface induces electron doping in FeSe [3, 4], leading to a distinct Fermi surface consisting of only two electron sheets around the corners of the tetragonal Brillouin zone (M point) [12]. The observed anisotropic superconducting gap has a more conventional form with plain s-wave symmetry [13] and is thus nodeless in the entire Brillouin zone. Furthermore, angular resolved photoemission spectroscopy (ARPES) measurements [6] reveal an interface-induced electron-phonon interaction between FeSe electrons and polar STO phonons that is strongly peaked at the $\mathbf{q}$=0 phonon wavevector [6, 14–16]. There is recent experimental evidence for the pivotal role of such interfacial phonons in engineering high-T_c heterostructures that involve FeSe [5, 9, 17] or even FeAs [18] monolayers.

Although *ab initio* calculations confirm the existence of small-q phonons as a strictly interfacial phenomenon in FeSe/STO [12, 19–21], the estimated low value of the electron-phonon coupling constant ($\lambda \leq 0.4$) has been commonly considered insufficient to explain the impressive T_c enhancement unless another, dominant pairing mechanism is at play [6]. However, a materials' specific theory of superconductivity that can account for the interplay between multiple bands, doping and small-q phonons has not yet been developed. It remains therefore unsolved to what extend and how such phonons contribute to the peculiar superconductivity in FeSe/STO.

Here, we present the first anisotropic, full bandwidth multiband Eliashberg calculations dedicated to unveil rigorously the influence of the interfacial electron-phonon coupling on superconductivity in FeSe/STO. Our self-consistent theory based solely on the interfacial electron-phonon coupling fully explains the high T_c and all enigmatic experimental observations, and allows us to unravel the mechanism of the high-T_c. Surprisingly, bands not crossing the Fermi level provide an additional Cooper pairing channel that enhances T_c and places the value of the gap over T_c ratio in the strong coupling regime.

The interface-induced electron-phonon interaction is modeled by a dispersionless mode at $\hbar\Omega$=81 meV [19] coupled to FeSe electrons via the functional form $g(\mathbf{q}) = g_0 \exp(-|\mathbf{q}|/q_c)$ with $q_c = 0.3a^{-1}$ [6], with a the FeSe lattice constant. This is the *only* mediator of superconductivity in our theory. For the electron dispersions of monolayer FeSe we use a recently derived ten-band tight-binding bandstructure [22]. Since the FeSe doping level is not *a priori* known, the electron filling is chosen such that the bottom of the electron bands around the M point in the Brillouin zone are at −50 meV as observed in experiment [2, 3, 6]. This leaves us with one free parameter, the electron-phonon scattering strength g_0, whose value we determine by requiring that the ARPES replica bands are reproduced at their observed energies [6]. We obtain $g_0 = 728$ meV which is remarkably close to the *ab initio* calculated value for anatase TiO_2 [23]. We solve the three coupled Eliashberg equations for $\Delta(\mathbf{k},\omega)$, $Z(\mathbf{k},\omega)$, and $\chi(\mathbf{k},\omega)$, describing the superconductivity order parameter, electron mass and chemical potential renormalizations, respectively, selfconsistently with full bandwidth, momentum and energy dependence; for details, see Supplementary Material (SM).

Figure 1(a) shows the calculated electron spectral function at T=10 K for the whole energy bandwidth and momenta along the M−Γ−M high-symmetry line of the folded Brillouin zone, which is measured in ARPES experiments. Comparison of the spectral function with the bare tight-binding band structure [22] used as input in our calculations (shown by white dashed lines) reveals that the interfacial small-q phonon modifies the FeSe

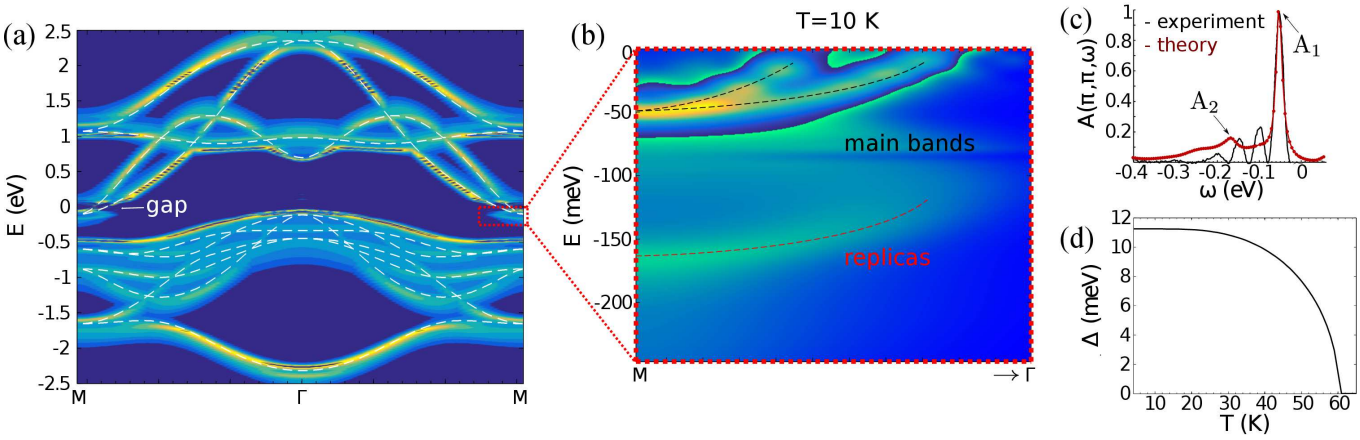

FIG. 1. Results of selfconsistent multiband Eliashberg theory calculations. (a) Calculated full bandwidth spectral function at 10 K, relevant to ARPES measurements, plotted along the M−Γ−M symmetry line of the Brillouin zone (BZ). The bare electron dispersions, used as input, are depicted by the white dashed lines. Several shake-off effects are visible in the quasiparticle band structure which are caused by interfacial electron-phonon interaction. (b) Spectral function for small energies near the M point [=(π,π)] of the BZ (red rectangle in a). Black dotted lines are guides to the eye. The formation of replica bands 110 meV deeper than the main electron bands is clearly resolved [6]. (c) The spectral function (red line) at M exhibits a main peak at −50 meV and an additional, weaker peak near −160 meV. The former peak is due to the main electron bands that form the Fermi surface in the normal state while the latter is their replica band contribution. The integrated experimental intensity at the M point [6] is shown by the black line. (d) Calculated temperature dependence of the superconducting gap edge maxima, giving $\Delta/k_{\rm B}T_{\rm c} \approx 2.1$.

electrons in a manifest way. Several shake-off effects in the band structure take place over the whole bandwidth, including the appearance of new bands near −160 meV. The opening of a superconducting gap around the Fermi level can be seen. Most of the predicted shake-off effects in the band structure have not yet been observed by experiment [24]. However, the replica bands appearing near the M point (zoom-in shown in Fig. 1(b)) at ∼110 meV distance from the main electron bands that form the Fermi surface have been experimentally resolved [6]. Figure 1(c) highlights that not only the position of the peaks but also the peak ratio, A_2/A_1=0.17, agrees well with experiment [6]. Notably, within solely phononic small-q theory we obtain the superconducting T_c=61 K, in good agreement with experiment [2, 6], with a temperature dependence of the gap edge as shown in Fig. 1(d). Thus, our selfconsistent calculations demonstrate that the interfacial electron-phonon coupling is responsible not only for the formation of the observed replica bands, but also for the high-T_c superconductivity in FeSe/STO, without the need of introducing additional boson mediators [6] such as spin fluctuations [25].

The momentum dependence of the calculated superconducting gap $\Delta(\mathbf{k}_{\rm F})$ is shown in Figure 2(a). It has s-wave symmetry and is moderately anisotropic (∼25%) with gap values that vary from 8−11 meV over the Fermi surface with an average value of 10 meV, in agreement with experiments [2, 6]. The resulting anisotropy of the gap is a consequence of the small-q form of the interfacial electron-phonon interaction (cf. [26]). Taking the maximum required excitation energy at the gap edge to calculate the gap over T_c ratio, we obtain the strong coupling (non-BCS) value $\Delta/k_{\rm B}T_{\rm c}$=2.1 (in contrast to the BCS value $\Delta/k_{\rm B}T_{\rm c}$=1.76). The chemical potential renor-

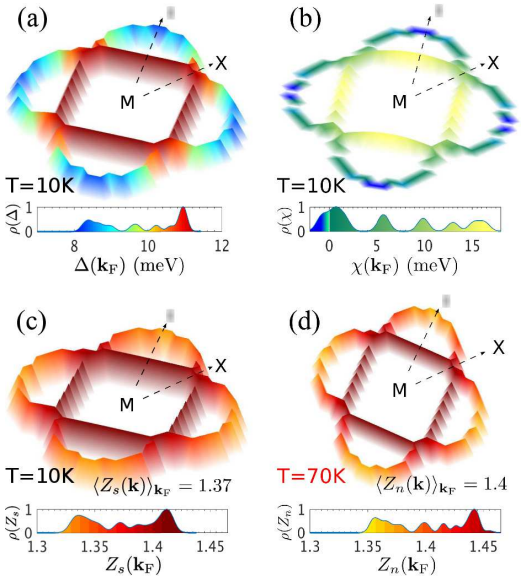

FIG. 2. Calculated momentum dependence of the superconducting gap and renormalization functions. (a) The gap edge $\Delta(\mathbf{k})$ is anisotropic (∼25%) over the Fermi surface with average value ∼10 meV. (b) The renormalized chemical potential $\chi(\mathbf{k})$ exhibits sign changes across the Fermi surface. (c) The mass renormalization function $Z(\mathbf{k})$ at T<T_c and (d) the same quantity at T>T_c. The insets show the distributions of the respective quantities over the Fermi surface.

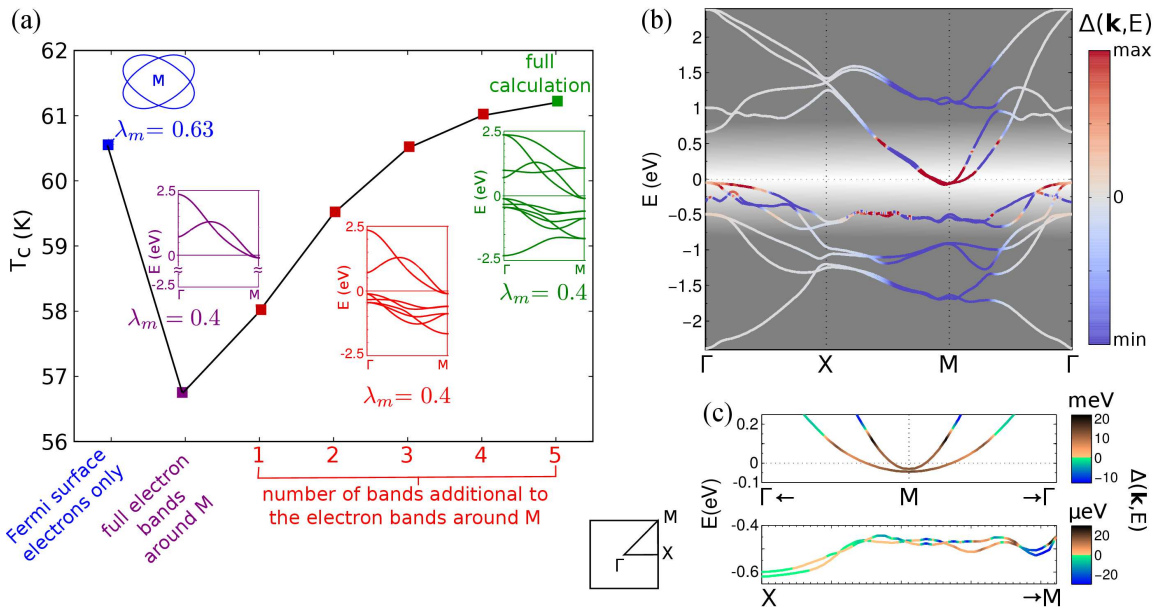

FIG. 3. Influence of included band dispersions on the superconductivity in monolayer FeSe/STO. (a) The calculated T_c, starting from electrons restricted only to the Fermi surface (blue) and subsequently including their full bandwidth (purple) and electron and hole (red) band contributions until the full ten band calculation is recovered (green). Spectral weight transfer to the replica bands weakens λ_m and therefore reduces T_c (purple). The interfacial phonon mode also couples weakly to bands away from the Fermi level, thus providing an additional channel to compensate this loss and even increase T_c (red and green). (b),(c) Cooper pair binding energy, $\Delta(\mathbf{k}, E)$, projected on each band of the renormalized electronic band structure due to the interfacial electron-phonon interaction. In (b) red (blue) color depicts electron attraction (repulsion) and thus Cooper pair formation (breaking). Apart from the dominant contribution of electrons in bands forming the Fermi surface (M point), deep Fermi-sea pairing takes place near the Γ point and along the X–M high symmetry line of the folded Brillouin zone.

malization $\chi(\mathbf{k}_F)$, shown in Fig. 2(b), has an anisotropic momentum dependence with an average Fermi surface value of $\langle\chi(\mathbf{k}_F)\rangle$=5.9 meV. The fact that $\chi(\mathbf{k}_F)$ even changes sign at certain Fermi surface points indicates the highly non-trivial role this quantity plays in shaping the quasiparticle band structure of the monolayer. In contrast, the mass renormalization function $Z(\mathbf{k}_F)$, shown in Figs. 2(c),(d) is rather isotropic with an average Fermi surface value $\langle Z(\mathbf{k}_F)\rangle$=1.37 and 1.40 for temperature below and above T_c, respectively. This quantity is related to the electron-phonon coupling constant λ_m, by $\langle Z(\mathbf{k})\rangle_{\mathbf{k}_F}|_{T>T_c}=1+\lambda_m$ which in our case yields λ_m= 0.4. This weak coupling value matches remarkably well to experiments [6, 10]. Also, in the superconducting state $\lambda_m^{10K}\approx$0.37 and satisfies $A_2/A_1\approx\lambda_m^{10K}/2$ (Fig. 1(c)) [27].

A plain calculation of T_c with our obtained value of λ_m=0.4 in McMillan's formula gives T_c=17 K. On the other hand, using our numerical results in the two T_c formulas recently proposed for interfacial phonon-mediated superconductivity in FeSe/STO [27, 28], yields T_c=272–283 K and 117.5 K, respectively. These estimations are in stark contrast to the T_c=61 K obtained here by our selfconsistent Eliashberg theory, which thus resolves the controversy between a seemingly weak λ_m and high-T_c superconductivity in FeSe/STO.

To elucidate further the mechanism of T_c enhancement in FeSe/STO, we carried out a series of simulations where we first solve the usual momentum-dependent Eliashberg equations for electrons only at the Fermi surface of FeSe/STO and then perform full-bandwidth calculations while sequentially adding more bands until we recover the full bandwidth multiband calculation. Our findings are summarized in Fig. 3(a). In the first case (blue symbol in Fig. 3(a)) where no electronic spectral rearrangement is allowed and thus no replica bands can form, we find λ_m=0.63. We note that this value equals the one given by the standard formula, $\lambda=\langle\lambda_{\mathbf{q}}\rangle_{\mathbf{k}_F,\mathbf{k}'_F}$=0.63 (with $\lambda_{\mathbf{q}}$ the momentum-dependent electron-phonon coupling). Therefore, the obtained T_c=60.6 K is the maximum T_c reachable by Fermi-surface Cooper pairing. Inclusion of the complete contribution of the two bands that form the Fermi surface (purple square in Fig. 3(a)) leads to λ_m=0.4 and T_c=56.8 K. Compared with the previous case, here a part of the electron-phonon coupling strength is consumed in mediating the electronic spectral weight transfer from the bands crossing the Fermi level to the replica bands. The effective interaction left available for Cooper-pair mediation is weaker and concomitantly so is the T_c. This weak coupling picture is further witnessed by the near-BCS value of the calculated ratio Δ/k_BT_c=1.8. Remarkably, turning on contributions from near-Fermi-level bands (red symbols in Fig. 3(a))

gradually increases T_c to 61.2 K (green square) but without affecting the value of λ_m. This behavior indicates that these bands do contribute to superconductivity.

To quantify this surprising conclusion, we projected the superconducting gap function $\Delta(\mathbf{k}, E)$ on the different electronic bands of FeSe/STO as shown in Fig. 3(b). Since $\Delta(\mathbf{k}, E)$ is a measure of the Cooper-pair binding energy, it is positive for Cooper pairing with an s-wave gap and negative otherwise [29]. Figure 3(b) clearly shows that superconductivity in FeSe/STO stems not only from Fermi surface regions around M, but also from regions around the Γ-X and X-M directions of the Brillouin zone. Although in the latter regions $\Delta(\mathbf{k}, E)$ is in the μeV range (Fig. 3(c)), the resulting net contribution is enough to overcompensate the T_c decreasing effect of the replica band formation. It is also enough to raise the Δ/k_BT_c ratio to 2.1 and thus provide a strong coupling phenomenology. Our findings thus generalize the usual BCS picture where Cooper pairing is restricted to Fermi surface electrons and prove that deep Fermi-sea Cooper pairing is possible in multiband systems. The recent puzzling superconductivity observed in doped LiFeAs without a Fermi surface [30] is plausibly explained within this picture.

Scanning tunneling spectroscopy (STS) measurements represent another key experimental feature reported for FeSe/STO [1, 13, 31]. To compare to STS data we have calculated the differential conductance spectrum dI/dV which, at low temperatures, is proportional to the superconducting density of states. The tunneling spectrum, calculated at T=10 K, is shown in Figure 4. Zooming-in to the low energy regime (Fig. 4(b)) reveals the opening of an s-wave superconducting gap in the tunneling spectra that starts to close already around ±5 meV and exhibits main coherence peaks at ±11 meV, with secondary peaks a few meV's higher. The calculated spectrum is in excellent agreement with STS measurements [1, 13, 31]. The position of the main coherence peaks in Fig. 4(b) coincides with the maximum of the gap-edge on the Fermi surface whereas the closing of the gap beginning at 5 meV is consistent with the minimum gap-edge of 8 meV (see Fig. 2(a)) in combination with the finite broadening of ∼3 meV used in our calculations.

Figure 4(a) shows the calculated tunneling spectra, normalized to the normal state values, at an intermediate energy range. Remarkably, we find superconductivity related structures in the spectrum up to energies almost 30 times higher than the superconducting gap itself. Although it is well established that such non-BCS behavior is the hallmark of strong-coupling superconductivity [29], this is unexpected here given the seemingly weak coupling constant of the system. In strongly coupled superconductors, the structure of the spectral function of the mediating bosons can be visible in the tunneling spectrum [29]. Here, we predict that the interfacial phonon mode should manifest itself as two kinks

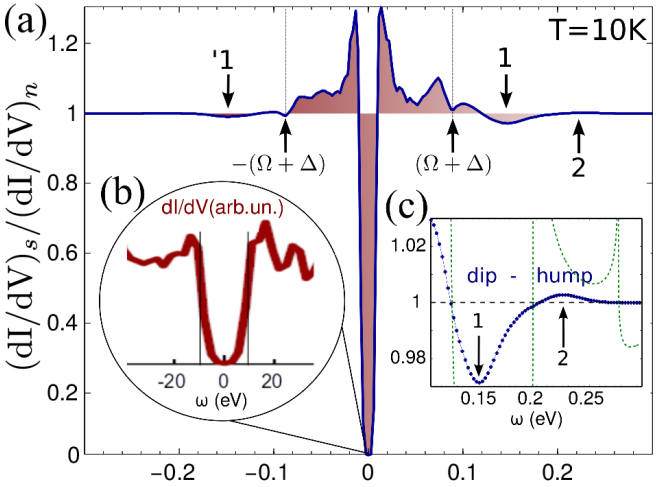

FIG. 4. Calculated tunneling spectra and predicted dip-hump signatures. (a) The differential conductance dI/dV in the energy regime relevant to superconductivity normalized by the normal state value. A full gap with main coherence peaks at $\Delta \approx \pm 11$ meV is in agreement with STS observations of plain s-wave superconductivity [13]. The kinks near $\pm(\Delta + \Omega) \approx \pm 91$ meV are signatures of the underlying electron-boson interaction, caused by the interfacial phonon mode. Additional features with the form of a dip-hump structure appear at higher energies, marked with 1('1) and 2, respectively. (b) The dI/dV in the low energy regime for direct comparison with STS data [13]. (c) A zoom-in of the dip-hump region of the normalized dI/dV reveals a dip with minima near 150 meV and a hump with maxima near 220 meV. Within standard isotropic Eliashberg theory (green dotted line), this dip-hump signature corresponds to a ratio $\Delta/k_BT_c \approx 2.1$ but with a strong coupling value of λ_{iso}=1.6.

around ±91 meV (Fig. 4(a)), whose location coincides with $\pm(\Omega + \Delta)$ where Δ is the average gap-edge value. Furthermore, at higher energies we predict a distinct dip-hump structure in the spectra with a dip at 150 meV and a hump at 220 meV (Figs. 4(a),(c)). Analyzing this additional strong coupling feature we find that it originates from the competition between the real and imaginary components of the superconducting gap function at an energy scale that is larger than the characteristic boson frequencies [32]. The energy location of the dip and the hump depends on the coupling strength [32], and more specifically, on the Δ/k_BT_c ratio. For comparison, within *isotropic* Eliashberg theory assuming an Einstein phonon at $\hbar\Omega$=81 meV, we find that our predicted dip-hump spectrum in FeSe/STO can only be fitted when the obtained gap over T_c ratio matches the one in FeSe/STO Δ/k_BT_c=2.1 but with a strong-coupling isotropic value λ_{iso}=1.6 (Fig. 4(c)).

Our first of its kind full-bandwidth multiband theory shows that the interfacial electron-phonon interaction in FeSe/STO with a seemingly weak λ_m=0.4 suffices to solely mediate the high-T_c superconductivity. Key experimental facts like the replica bands, superconducting

gap and tunneling spectra are all meticulously explained within our materials specific framework. A definite confirmation for this scenario will be the observation of a dip-hump feature in the tunneling spectra. Our explicit calculations unveil the T_c increasing effect of deep Fermi-sea Cooper pairing and the T_c decreasing effect of replica-band formation, and suggest new pathways to engineer high T_c's. On a fundamental level, our findings put to the question the current standard perception of the efficiency of electron-phonon interaction in mediating high-T_c superconductivity and, whether Fermi-surface restricted theory is sufficient to capture the superconductivity of other doped high-T_c materials.

* alex.aperis@physics.uu.se
† peter.oppeneer@physics.uu.se

[1] W. Qing-Yan, L. Zhi, Z. Wen-Hao, Z. Zuo-Cheng, Z. Jin-Song, L. Wei, D. Hao, O. Yun-Bo, D. Peng, C. Kai, W. Jing, S. Can-Li, H. Ke, J. Jin-Feng, J. Shuai-Hua, W. Ya-Yu, W. Li-Li, C. Xi, M. Xu-Cun, and X. Qi-Kun, Chin. Phys. Lett. **29**, 037402 (2012).
[2] D. Liu, W. Zhang, D. Mou, J. He, Y.-B. Ou, Q.-Y. Wang, Z. Li, L. Wang, L. Zhao, S. He, Y. Peng, X. Liu, C. Chen, L. Yu, G. Liu, X. Dong, J. Zhang, C. Chen, Z. Xu, J. Hu, X. Chen, X. Ma, Q. Xue, and X. Zhou, Nat. Commun. **3**, 931 (2012).
[3] S. He, J. He, W. Zhang, L. Zhao, D. Liu, X. Liu, D. Mou, Y.-B. Ou, Q.-Y. Wang, Z. Li, L. Wang, Y. Peng, Y. Liu, C. Chen, L. Yu, G. Liu, X. Dong, J. Zhang, C. Chen, Z. Xu, X. Chen, X. Ma, Q. Xue, and X. J. Zhou, Nat. Mater. **12**, 605 (2013).
[4] S. Tan, Y. Zhang, M. Xia, Z. Ye, F. Chen, X. Xie, R. Peng, D. Xu, Q. Fan, H. Xu, J. Jiang, T. Zhang, X. Lai, T. Xiang, J. Hu, B. Xie, and D. Feng, Nat. Mater. **12**, 634 (2013).
[5] R. Peng, H. C. Xu, S. Y. Tan, H. Y. Cao, M. Xia, X. P. Shen, Z. C. Huang, C. Wen, Q. Song, T. Zhang, B. P. Xie, X. G. Gong, and D. L. Feng, Nat. Commun. **5**, 5044 (2014).
[6] J. J. Lee, F. T. Schmitt, R. G. Moore, S. Johnston, Y.-T. Cui, W. Li, M. Yi, Z. K. Liu, M. Hashimoto, Y. Zhang, D. H. Lu, T. P. Devereaux, D.-H. Lee, and Z.-X. Shen, Nature **515**, 245 (2014).
[7] J.-F. Ge, Z.-L. Liu, C. Liu, C.-L. Gao, D. Qian, Q.-K. Xue, Y. Liu, and J.-F. Jia, Nat. Mater. **14**, 285 (2015).
[8] F.-C. Hsu, J.-Y. Luo, K.-W. Yeh, T.-K. Chen, T.-W. Huang, P. M. Wu, Y.-C. Lee, Y.-L. Huang, Y.-Y. Chu, D.-C. Yan, and M.-K. Wu, Proc. Natl. Acad. Sci. USA **105**, 14262 (2008).
[9] H. Ding, Y.-F. Lv, K. Zhao, W.-L. Wang, L. Wang, C.-L. Song, X. Chen, X.-C. Ma, and Q.-K. Xue, Phys. Rev. Lett. **117**, 067001 (2016).
[10] Y. C. Tian, W. H. Zhang, F. S. Li, Y. L. Wu, Q. Wu, F. Sun, G. Y. Zhou, L. Wang, X. Ma, Q.-K. Xue, and J. Zhao, Phys. Rev. Lett. **116**, 107001 (2016).
[11] I. I. Mazin, D. J. Singh, M. D. Johannes, and M. H. Du, Phys. Rev. Lett. **101**, 057003 (2008).
[12] B. Li, Z. W. Xing, G. Q. Huang, and D. Y. Xing, J. Appl. Phys. **115**, 193907 (2014).
[13] Q. Fan, W. H. Zhang, X. Liu, Y. J. Yan, M. Q. Ren, R. Peng, H. C. Xu, B. P. Xie, J. P. Hu, T. Zhang, and D. L. Feng, Nat. Phys. **11**, 946 (2015).
[14] A. Aperis, P. Kotetes, G. Varelogiannis, and P. M. Oppeneer, Phys. Rev. B **83**, 092505 (2011).
[15] M. Weger and M. Peter, Physica C: Superconductivity **317 - 318**, 252 (1999).
[16] A. A. Abrikosov, Physica C: Superconductivity **222**, 191 (1994).
[17] S. N. Rebec, T. Jia, C. Zhang, M. Hashimoto, D.-H. Lu, R. G. Moore, and Z.-X. Shen, ArXiv e-prints (2016), arXiv:1606.09358 [cond-mat.supr-con].
[18] S. Choi, W.-J. Jang, H.-J. Lee, J. M. Ok, H. W. Choi, A. Taekyung Lee, A. Akbari, H. Suh, Y. K. Semertzidis, Y. Bang, J. S. Kim, and J. Lee, ArXiv e-prints (2016), arXiv:1608.00886 [cond-mat.supr-con].
[19] Y. Xie, H.-Y. Cao, Y. Zhou, S. Chen, H. Xiang, and X.-G. Gong, Scie. Rep. **5**, 10011 (2015).
[20] Y. Wang, A. Linscheid, T. Berlijn, and S. Johnston, Phys. Rev. B **93**, 134513 (2016).
[21] Y. Zhou and A. J. Millis, Phys. Rev. B **93**, 224506 (2016).
[22] N. Hao and J. Hu, Phys. Rev. X **4**, 031053 (2014).
[23] C. Verdi and F. Giustino, Phys. Rev. Lett. **115**, 176401 (2015).
[24] Y. Wang, K. Nakatsukasa, L. Rademaker, T. Berlijn, and S. Johnston, Superconductor Science and Technology **29**, 054009 (2016).
[25] A. Linscheid, S. Maiti, Y. Wang, S. Johnston, and P. J. Hirschfeld, Phys. Rev. Lett. **117**, 077003 (2016).
[26] G. Varelogiannis, A. Perali, E. Cappelluti, and L. Pietronero, Phys. Rev. B **54**, R6877 (1996).
[27] M. L. Kulić and O. V. Dolgov, New Journal of Physics **19**, 013020 (2017).
[28] L. Rademaker, Y. Wang, T. Berlijn, and S. Johnston, New J. Phys. **18**, 022001 (2016).
[29] D. J. Scalapino, J. R. Schrieffer, and J. W. Wilkins, Phys. Rev. **148**, 263 (1966).
[30] H. Miao, T. Qian, X. Shi, P. Richard, T. K. Kim, M. Hoesch, L. Y. Xing, X.-C. Wang, C.-Q. Jin, J.-P. Hu, and H. Ding, Nat. Commun. **6**, 6056 (2015).
[31] C. Tang, C. Liu, G. Zhou, F. Li, H. Ding, Z. Li, D. Zhang, Z. Li, C. Song, S. Ji, K. He, L. Wang, X. Ma, and Q.-K. Xue, Phys. Rev. B **93**, 020507 (2016).
[32] G. Varelogiannis, Phys. Rev. B **51**, 1381 (1995).

Acknowledgements
We thank G. Varelogiannis for fruitful discussions. This work has been supported by the Swedish Research Council (VR), the Röntgen-Ångström Cluster, and the Swedish National Infrastructure for Computing (SNIC).

SUPPLEMENTARY MATERIAL

Our starting point is the general Hamiltonian that accounts for the monolayer FeSe electrons, the interface-induced small-q phonon mode, and their mutual coupling. The full electron dispersions of the monolayer FeSe are described by a realistic, ten band tight-binding band structure [22] that is based on Density Functional Theory (DFT) calculations. In addition, we allow for the interface-induced phonon to couple with electrons from all bands on the same footing. Consequently, the resulting Migdal-Eliashberg equations couple all ten bands. The resulting momentum-dependent Eliashberg function has a separable form in frequency/momentum domain and this feature is inherent to the electron-phonon coupling, as well. However, due to the full bandwidth nature of our calculation, the obtained solutions to the Eliashberg equations are non-separable in momentum and frequency. By including superconductivity as a possible self-consistent solution in the Eliashberg equations, we treat the full problem of the FeSe monolayer in a selfconsistent manner. Since $g(\mathbf{q})$ is band independent, we are left with solving for the global matrix electron self-energy

$$\hat{\Sigma}(\mathbf{k}, i\omega_m) = T \sum_{\mathbf{k}', m'} \sum_{n} \hat{\tau}_3 \hat{G}_n(\mathbf{k}', i\omega_{m'}) \hat{\tau}_3 g^2_{\mathbf{q}} f_{mm'} \quad (1)$$

where $n = 1, \ldots, 10$ indexes the electron bands, $\omega_m = \pi \mathrm{T}(2m+1)$ are fermion Matsubara frequencies, $\hat{\tau}_i$ are Pauli matrices in Nambu space, and $f_{mm'}$ is the Matsubara frequency dependent part of the electron-phonon interaction. The system is far from half filling, therefore standard Eliashberg treatment where the electronic degrees of freedom away from the Fermi surface are integrated out cannot be applied here and the full bandwidth, fully anisotropic, multiband problem needs to be solved instead. The matrix Green function for each band

$$\begin{aligned} \hat{G}_n^{-1}(\mathbf{k}, i\omega_m) = i\omega_m Z(\mathbf{k}, i\omega_m) - [\xi_n(\mathbf{k}) + \chi(\mathbf{k}, i\omega_m)]\hat{\tau}_3 \\ - \Delta(\mathbf{k}, i\omega_m) Z(\mathbf{k}, i\omega_m) \hat{\tau}_1 \end{aligned} \quad (2)$$

includes except from the mass renormalization function $Z(\mathbf{k}, i\omega_m)$ and the superconducting part $\Delta(\mathbf{k}, i\omega_m)$, the chemical potential term $\chi(\mathbf{k}, i\omega_m)$ which acts as a momentum- and frequency-dependent energy shift for the electrons due to the electron-phonon interaction. The resulting coupled Eliashberg equations are solved self-consistently in the folded Brillouin zone and then are analytically continued for real frequencies with a self-consistent analytic continuation technique. For such demanding calculations, the cutoff frequency in the Matsubara sums needs to be extended up to the bandwidth. We have checked that cutoffs smaller than that can crucially distort the final results after the analytic continuation. Thus, in the calculations presented here, we used a 128x128 k-point mesh and up to 4000 Matsubara frequencies.